

Search for $\Lambda_c^+ \rightarrow \phi p \pi^0$ and branching fraction measurement of $\Lambda_c^+ \rightarrow K^- \pi^+ p \pi^0$

B. Pal,⁶ A. J. Schwartz,⁶ I. Adachi,^{14,10} H. Aihara,⁷¹ S. Al Said,^{65,32} D. M. Asner,⁵⁶ T. Aushev,⁴⁵ R. Ayad,⁶⁵ I. Badhrees,^{65,31} A. M. Bakich,⁶⁴ V. Bansal,⁵⁶ P. Behera,¹⁹ M. Berger,⁶² V. Bhardwaj,⁷⁹ J. Biswal,²⁷ A. Bobrov,^{3,54} A. Bozek,⁵¹ M. Bračko,^{41,27} T. E. Browder,¹³ D. Červenkov,⁴ V. Chekelian,⁴² A. Chen,⁴⁸ B. G. Cheon,¹² K. Chilikin,^{38,44} K. Cho,³³ S.-K. Choi,¹¹ Y. Choi,⁶³ D. Cinabro,⁷⁶ N. Dash,¹⁷ S. Di Carlo,⁷⁶ Z. Doležal,⁴ Z. Drásal,⁴ S. Eidelman,^{3,54} T. Ferber,⁷ B. G. Fulsom,⁵⁶ V. Gaur,⁷⁵ N. Gabyshev,^{3,54} A. Garmash,^{3,54} P. Goldenzweig,²⁹ E. Guido,²⁵ T. Hara,^{14,10} K. Hayasaka,⁵³ H. Hayashii,⁴⁷ W.-S. Hou,⁵⁰ C.-L. Hsu,⁴³ K. Inami,⁴⁶ A. Ishikawa,⁷⁰ R. Itoh,^{14,10} W. W. Jacobs,²⁰ I. Jaegle,⁸ H. B. Jeon,³⁶ S. Jia,² Y. Jin,⁷¹ D. Joffe,³⁰ K. K. Joo,⁵ G. Karyan,⁷ Y. Kato,⁴⁶ D. Y. Kim,⁶¹ J. B. Kim,³⁴ K. T. Kim,³⁴ S. H. Kim,¹² Y. J. Kim,³³ K. Kinoshita,⁶ P. Kodyš,⁴ S. Korpar,^{41,27} D. Kotchetkov,¹³ P. Krokovny,^{3,54} T. Kuhr,³⁹ R. Kulasiri,³⁰ Y.-J. Kwon,⁷⁸ C. H. Li,⁴³ L. Li,⁵⁹ Y. Li,⁷⁵ L. Li Gioi,⁴² J. Libby,¹⁹ D. Liventsev,^{75,14} M. Lubej,²⁷ T. Luo,⁵⁷ J. MacNaughton,¹⁴ D. Matvienko,^{3,54} M. Merola,²⁴ K. Miyabayashi,⁴⁷ H. Miyata,⁵³ R. Mizuk,^{38,44,45} G. B. Mohanty,⁶⁶ H. K. Moon,³⁴ T. Mori,⁴⁶ R. Mussa,²⁵ E. Nakano,⁵⁵ M. Nakao,^{14,10} T. Nanut,²⁷ K. J. Nath,¹⁸ M. Nayak,^{76,14} M. Niiyama,³⁵ S. Nishida,^{14,10} S. Ogawa,⁶⁹ H. Ono,^{52,53} P. Pakhlov,^{38,44} G. Pakhlova,^{38,45} S. Pardi,²⁴ C.-S. Park,⁷⁸ S. Paul,⁶⁸ T. K. Pedlar,⁴⁰ R. Pestotnik,²⁷ L. E. Piilonen,⁷⁵ M. Ritter,³⁹ A. Rostomyan,⁷ Y. Sakai,^{14,10} S. Sandilya,⁶ L. Santelj,¹⁴ T. Sanuki,⁷⁰ V. Savinov,⁵⁷ O. Schneider,³⁷ G. Schnell,^{1,16} C. Schwanda,²² Y. Seino,⁵³ K. Senyo,⁷⁷ M. E. Sevier,⁴³ T.-A. Shibata,⁷² J.-G. Shiu,⁵⁰ F. Simon,^{42,67} A. Sokolov,²³ E. Solovieva,^{38,45} M. Starič,²⁷ J. F. Strube,⁵⁶ M. Sumihama,⁹ T. Sumiyoshi,⁷³ M. Takizawa,^{60,15,58} U. Tamponi,^{25,74} K. Tanida,²⁶ F. Tenchini,⁴³ M. Uchida,⁷² T. Uglov,^{38,45} S. Uno,^{14,10} C. Van Hulse,¹ G. Varner,¹³ K. E. Varvell,⁶⁴ A. Vinokurova,^{3,54} V. Vorobyev,^{3,54} C. H. Wang,⁴⁹ M.-Z. Wang,⁵⁰ X. L. Wang,^{56,14} M. Watanabe,⁵³ Y. Watanabe,²⁸ S. Watanuki,⁷⁰ E. Widmann,⁶² E. Won,³⁴ Y. Yamashita,⁵² H. Ye,⁷ J. Yelton,⁸ C. Z. Yuan,²¹ Z. P. Zhang,⁵⁹ V. Zhilich,^{3,54} V. Zhukova,⁴⁴ V. Zhulanov,^{3,54} and A. Zupanc^{80,27}

(The Belle Collaboration)

¹University of the Basque Country UPV/EHU, 48080 Bilbao

²Beihang University, Beijing 100191

³Budker Institute of Nuclear Physics SB RAS, Novosibirsk 630090

⁴Faculty of Mathematics and Physics, Charles University, 121 16 Prague

⁵Chonnam National University, Kwangju 660-701

⁶University of Cincinnati, Cincinnati, Ohio 45221

⁷Deutsches Elektronen-Synchrotron, 22607 Hamburg

⁸University of Florida, Gainesville, Florida 32611

⁹Gifu University, Gifu 501-1193

¹⁰SOKENDAI (The Graduate University for Advanced Studies), Hayama 240-0193

¹¹Gyeongsang National University, Chinju 660-701

¹²Hanyang University, Seoul 133-791

¹³University of Hawaii, Honolulu, Hawaii 96822

¹⁴High Energy Accelerator Research Organization (KEK), Tsukuba 305-0801

¹⁵J-PARC Branch, KEK Theory Center, High Energy Accelerator Research Organization (KEK), Tsukuba 305-0801

¹⁶IKERBASQUE, Basque Foundation for Science, 48013 Bilbao

¹⁷Indian Institute of Technology Bhubaneswar, Satya Nagar 751007

¹⁸Indian Institute of Technology Guwahati, Assam 781039

¹⁹Indian Institute of Technology Madras, Chennai 600036

²⁰Indiana University, Bloomington, Indiana 47408

²¹Institute of High Energy Physics, Chinese Academy of Sciences, Beijing 100049

²²Institute of High Energy Physics, Vienna 1050

²³Institute for High Energy Physics, Protvino 142281

²⁴INFN - Sezione di Napoli, 80126 Napoli

²⁵INFN - Sezione di Torino, 10125 Torino

²⁶Advanced Science Research Center, Japan Atomic Energy Agency, Naka 319-1195

²⁷J. Stefan Institute, 1000 Ljubljana

²⁸Kanagawa University, Yokohama 221-8686

²⁹Institut für Experimentelle Kernphysik, Karlsruher Institut für Technologie, 76131 Karlsruhe

³⁰Kennesaw State University, Kennesaw, Georgia 30144

- ³¹King Abdulaziz City for Science and Technology, Riyadh 11442
- ³²Department of Physics, Faculty of Science, King Abdulaziz University, Jeddah 21589
- ³³Korea Institute of Science and Technology Information, Daejeon 305-806
- ³⁴Korea University, Seoul 136-713
- ³⁵Kyoto University, Kyoto 606-8502
- ³⁶Kyungpook National University, Daegu 702-701
- ³⁷École Polytechnique Fédérale de Lausanne (EPFL), Lausanne 1015
- ³⁸P.N. Lebedev Physical Institute of the Russian Academy of Sciences, Moscow 119991
- ³⁹Ludwig Maximilians University, 80539 Munich
- ⁴⁰Luther College, Decorah, Iowa 52101
- ⁴¹University of Maribor, 2000 Maribor
- ⁴²Max-Planck-Institut für Physik, 80805 München
- ⁴³School of Physics, University of Melbourne, Victoria 3010
- ⁴⁴Moscow Physical Engineering Institute, Moscow 115409
- ⁴⁵Moscow Institute of Physics and Technology, Moscow Region 141700
- ⁴⁶Graduate School of Science, Nagoya University, Nagoya 464-8602
- ⁴⁷Nara Women's University, Nara 630-8506
- ⁴⁸National Central University, Chung-li 32054
- ⁴⁹National United University, Miao Li 36003
- ⁵⁰Department of Physics, National Taiwan University, Taipei 10617
- ⁵¹H. Niewodniczanski Institute of Nuclear Physics, Krakow 31-342
- ⁵²Nippon Dental University, Niigata 951-8580
- ⁵³Niigata University, Niigata 950-2181
- ⁵⁴Novosibirsk State University, Novosibirsk 630090
- ⁵⁵Osaka City University, Osaka 558-8585
- ⁵⁶Pacific Northwest National Laboratory, Richland, Washington 99352
- ⁵⁷University of Pittsburgh, Pittsburgh, Pennsylvania 15260
- ⁵⁸Theoretical Research Division, Nishina Center, RIKEN, Saitama 351-0198
- ⁵⁹University of Science and Technology of China, Hefei 230026
- ⁶⁰Showa Pharmaceutical University, Tokyo 194-8543
- ⁶¹Soongsil University, Seoul 156-743
- ⁶²Stefan Meyer Institute for Subatomic Physics, Vienna 1090
- ⁶³Sungkyunkwan University, Suwon 440-746
- ⁶⁴School of Physics, University of Sydney, New South Wales 2006
- ⁶⁵Department of Physics, Faculty of Science, University of Tabuk, Tabuk 71451
- ⁶⁶Tata Institute of Fundamental Research, Mumbai 400005
- ⁶⁷Excellence Cluster Universe, Technische Universität München, 85748 Garching
- ⁶⁸Department of Physics, Technische Universität München, 85748 Garching
- ⁶⁹Toho University, Funabashi 274-8510
- ⁷⁰Department of Physics, Tohoku University, Sendai 980-8578
- ⁷¹Department of Physics, University of Tokyo, Tokyo 113-0033
- ⁷²Tokyo Institute of Technology, Tokyo 152-8550
- ⁷³Tokyo Metropolitan University, Tokyo 192-0397
- ⁷⁴University of Torino, 10124 Torino
- ⁷⁵Virginia Polytechnic Institute and State University, Blacksburg, Virginia 24061
- ⁷⁶Wayne State University, Detroit, Michigan 48202
- ⁷⁷Yamagata University, Yamagata 990-8560
- ⁷⁸Yonsei University, Seoul 120-749
- ⁷⁹Indian Institute of Science Education and Research Mohali, SAS Nagar, 140306
- ⁸⁰Faculty of Mathematics and Physics, University of Ljubljana, 1000 Ljubljana

We have searched for the Cabibbo-suppressed decay $\Lambda_c^+ \rightarrow \phi p \pi^0$ in e^+e^- collisions using a data sample corresponding to an integrated luminosity of 915 fb^{-1} . The data were collected by the Belle experiment at the KEKB e^+e^- asymmetric-energy collider running at or near the $\Upsilon(4S)$ and $\Upsilon(5S)$ resonances. No significant signal is observed, and we set an upper limit on the branching fraction of $\mathcal{B}(\Lambda_c^+ \rightarrow \phi p \pi^0) < 15.3 \times 10^{-5}$ at 90% confidence level. The contribution of nonresonant $\Lambda_c^+ \rightarrow K^+ K^- p \pi^0$ decays is found to be consistent with zero, and the corresponding upper limit on its branching fraction is set to be $\mathcal{B}(\Lambda_c^+ \rightarrow K^+ K^- p \pi^0)_{\text{NR}} < 6.3 \times 10^{-5}$ at 90% confidence level. We also search for an intermediate hidden-strangeness pentaquark decay $P_s^+ \rightarrow \phi p$. We see no evidence for this intermediate decay and set an upper limit on the product branching fraction of $\mathcal{B}(\Lambda_c^+ \rightarrow P_s^+ \pi^0) \times \mathcal{B}(P_s^+ \rightarrow \phi p) < 8.3 \times 10^{-5}$ at 90% confidence level. Finally, we measure the branching fraction for the Cabibbo-favored decay $\Lambda_c^+ \rightarrow K^- \pi^+ p \pi^0$; the result is $\mathcal{B}(\Lambda_c^+ \rightarrow K^- \pi^+ p \pi^0) = (4.42 \pm 0.05 \text{ (stat.)} \pm 0.12 \text{ (syst.)} \pm 0.16 \text{ (norm.)})\%$, which is the most precise measurement to date.

The story of exotic hadron spectroscopy begins with the discovery of the $X(3872)$ by the Belle collaboration in 2003 [1]. Since then, many exotic XYZ states have been reported by Belle and other experiments [2]. Recent observations of two hidden-charm pentaquark states $P_c^+(4380)$ and $P_c^+(4450)$ by the LHCb collaboration in the $J/\psi p$ invariant mass spectrum of the $\Lambda_b^0 \rightarrow J/\psi p K^-$ process [3] raises the question of whether a hidden-strangeness pentaquark P_s^+ , where the $c\bar{c}$ pair in P_c^+ is replaced by an $s\bar{s}$ pair, exists [4–6]. The strange-flavor analogue of the P_c^+ discovery channel is the decay $\Lambda_c^+ \rightarrow \phi p \pi^0$ [5, 6], shown in Fig. 1 (a) [7]. The detection of a hidden-strangeness pentaquark could be possible through the ϕp invariant mass spectrum within this channel [see Fig. 1 (b)], if the underlying mechanism creating the P_c^+ states also holds for P_s^+ , independent of the flavor [6], and only if the mass of P_s^+ is less than $M_{\Lambda_c^+} - M_{\pi^0}$. In an analogous $s\bar{s}$ process of ϕ photoproduction ($\gamma p \rightarrow \phi p$), a forward-angle bump structure at $\sqrt{s} \approx 2.0$ GeV has been observed by the LEPS [8] and CLAS collaborations [9]. However, this structure appears only at the most forward angles, which is not expected for the decay of a resonance [10].

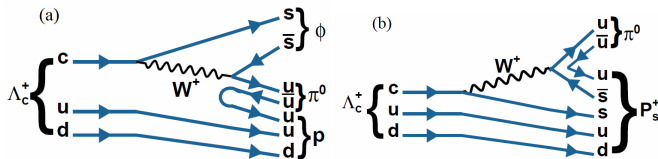


FIG. 1. Feynman diagram for the decay (a) $\Lambda_c^+ \rightarrow \phi p \pi^0$ and (b) $\Lambda_c^+ \rightarrow P_s^+ \pi^0$.

Previously, the decay $\Lambda_c^+ \rightarrow \phi p \pi^0$ has not been studied by any experiment. In this paper, we report a search for this decay using a data set corresponding to an integrated luminosity of 915 fb^{-1} collected with the Belle detector [11] recorded at or near the $\Upsilon(4S)$ and $\Upsilon(5S)$ resonances at the KEKB asymmetric-energy e^+e^- (3.5 on 8.0 GeV) collider [12]. In addition, we search for the nonresonant decay $\Lambda_c^+ \rightarrow K^+ K^- p \pi^0$ and measure the branching fraction of the Cabibbo-favored decay $\Lambda_c^+ \rightarrow K^- \pi^+ p \pi^0$.

The Belle detector is described in detail elsewhere [11]. To calculate the detector acceptance and reconstruction efficiencies and to study background, we use Monte Carlo (MC) simulated events. The MC events are generated uniformly in phase space with EVTGEN [13] and JETSET [14]; the detector response is modeled using GEANT3 [15]. Final-state radiation is taken into account using the PHOTOS [16] package.

The reconstruction of $\Lambda_c^+ \rightarrow \phi p \pi^0$ (and $\Lambda_c^+ \rightarrow K^- \pi^+ p \pi^0$) decays proceeds by first reconstructing $\pi^0 \rightarrow$

$\gamma\gamma$ candidates. An electromagnetic calorimeter (ECL) cluster not matched to any track is identified as a photon candidate. Such candidates are required to have an energy greater than 50 MeV in the barrel region and 100 MeV in the endcap regions, where the barrel region covers the polar angle range $32^\circ < \theta < 130^\circ$, and the endcap regions cover the ranges $12^\circ < \theta < 32^\circ$ and $130^\circ < \theta < 157^\circ$. To reject showers produced by neutral hadrons, the photon energy deposited in the 3×3 array of ECL crystals centered on the crystal with the highest energy must exceed 80% of the energy deposited in the corresponding 5×5 array of crystals. We require that the $\gamma\gamma$ invariant mass be within $0.020 \text{ GeV}/c^2$ (about 3.5σ in resolution) of the known π^0 mass [17]. To improve the π^0 momentum resolution, we perform a mass-constrained fit and require that the resulting χ^2 be less than 30. In addition, the momentum of the π^0 candidates in the center-of-mass (CM) frame is required to be higher than $0.30 \text{ GeV}/c$.

We subsequently combine π^0 candidates with three charged tracks. Such tracks are identified using requirements on the distance of closest approach with respect to the interaction point along the z axis (antiparallel to the e^+ beam) of $|dz| < 1.0 \text{ cm}$, and in the transverse plane of $dr < 0.1 \text{ cm}$. In addition, charged tracks are required to have a minimum number of hits in the vertex detector (> 1 in both the z and transverse directions). Information obtained from the central drift chamber, the time-of-flight scintillation counters, and the aerogel threshold Cherenkov counters is combined to form a likelihood \mathcal{L} for hadron identification. A charged track with the likelihood ratios of $\mathcal{L}_K/(\mathcal{L}_\pi + \mathcal{L}_K) > 0.9$ and $\mathcal{L}_K/(\mathcal{L}_p + \mathcal{L}_K) > 0.6$; $\mathcal{L}_K/(\mathcal{L}_\pi + \mathcal{L}_K) < 0.6$ and $\mathcal{L}_\pi/(\mathcal{L}_p + \mathcal{L}_\pi) > 0.6$; and $\mathcal{L}_p/(\mathcal{L}_p + \mathcal{L}_K) > 0.9$ and $\mathcal{L}_p/(\mathcal{L}_p + \mathcal{L}_\pi) > 0.9$ is regarded as kaon, pion and proton, respectively. The efficiencies of these requirements for kaons, pions, and protons are 77%, 97%, and 75%, respectively. The probabilities for a kaon, pion, or proton to be misidentified are $\mathcal{P}(K \rightarrow \pi) \approx 10\%$, $\mathcal{P}(K \rightarrow p) \approx 1\%$; $\mathcal{P}(\pi \rightarrow K) \approx 1\%$, $\mathcal{P}(\pi \rightarrow p) < 1\%$; and $\mathcal{P}(p \rightarrow K) \approx 7\%$, $\mathcal{P}(p \rightarrow \pi) \approx 1\%$. Candidate ϕ mesons are formed from two oppositely charged tracks that have been identified as kaons. We accept events in the wide K^+K^- mass range $m(K^+K^-) \in (0.99, 1.13) \text{ GeV}/c^2$. To suppress combinatorial background, especially from B meson decays, we require that the scaled momentum ($x_p = Pc/\sqrt{E_{\text{CM}}^2/4 - M^2c^4}$) be greater than 0.45, where E_{CM} is the total CM energy, and P and M are the momentum and invariant mass of the Λ_c^+ candidates. A vertex fit is performed to the charged tracks to form a Λ_c^+ vertex, and we require that the χ^2 from the fit be less than 50. The decay $\Lambda_c^+ \rightarrow \Sigma^+ \phi$ has the same final state as the signal decay and is Cabibbo-favored. To

avoid contamination from this decay, we reject candidates in which the $p\pi^0$ system has an invariant mass within 0.010 GeV/ c^2 of the known Σ^+ mass [17]. We extract the Λ_c^+ yield in a signal region that spans 2.5σ in resolution around the Λ_c^+ mass [17]; this range corresponds to ± 0.015 GeV/ c^2 for $\Lambda_c \rightarrow K^-\pi^+p\pi^0$ and approximately ± 0.010 GeV/ c^2 for the other decays studied.

After applying all these selection criteria, about 16% of events in the signal region have multiple Λ_c^+ candidates. For these events, we retain the candidate having the smallest sum of χ^2 values obtained from the π^0 mass-constrained fit and the Λ_c^+ vertex fit. According to MC simulation, this criterion selects the correct Λ_c^+ candidate in 72% of multiple-candidate events.

In order to extract the signal yield, we perform a two-dimensional (2D) unbinned extended maximum likelihood fit to the variables $m(K^+K^-p\pi^0)$ and $m(K^+K^-)$. Our likelihood function accounts for three components: $\phi p\pi^0$ signal, $K^+K^-p\pi^0$ nonresonant events, and combinatorial background. The likelihood function is defined as

$$e^{-\sum_j Y_j} \prod_i^N \left(\sum_j Y_j \mathcal{P}_j [m^i(K^+K^-p\pi^0), m^i(K^+K^-)] \right), \quad (1)$$

where N is the total number of events, $\mathcal{P}_j [m^i(K^+K^-p\pi^0), m^i(K^+K^-)]$ is the probability density function (PDF) of signal or background component j for event i , and j runs over all signal and background components. The parameter Y_j is the yield of component j . The $m(K^+K^-p\pi^0)$ for signal and nonresonant contributions are modeled with the sum of two Crystal Ball (CB) functions [18] having a common mean, whereas for the combinatorial background, a second-order Chebyshev polynomial is used. The peak positions and resolutions of the CB functions are adjusted according to data-MC differences observed in the high statistics sample of $\Lambda_c^+ \rightarrow K^-\pi^+p\pi^0$ decays. The $m(K^+K^-)$ of signal is modeled with a relativistic Breit-Wigner function convolved with a Gaussian resolution function (RBW \otimes G), with the mass and width of the resonance ϕ fixed to their nominal values [17]. The width of the Gaussian resolution function is fixed to the value obtained from the MC simulation. The $m(K^+K^-)$ of nonresonant background is modeled with a one-dimensional nonparametric PDF [19]. The $m(K^+K^-)$ of combinatorial background is modeled with the sum of a third-order Chebyshev polynomial and the same RBW \otimes G function as used to model the signal. The floated parameters are the component yields Y_j and, for the combinatorial background, the coefficients of the Chebyshev polynomials and the fraction of the RBW. All other parameters are fixed in the fit to the values obtained from the MC simulation. Projections of the fit result are shown in Fig. 2. From the fit, we extract

148.4 ± 61.8 signal events, 75.9 ± 84.8 nonresonant events, and 7158.4 ± 36.4 combinatorial background events in the Λ_c^+ signal region. The statistical significance is evaluated as $\sqrt{-2 \ln(\mathcal{L}_0/\mathcal{L}_{\max})}$, where \mathcal{L}_0 is the likelihood value when the signal yield is fixed to zero, and \mathcal{L}_{\max} is the nominal likelihood value. The statistical significances are found to be 2.4 and 1.0 standard deviations for $\Lambda_c^+ \rightarrow \phi p\pi^0$ and nonresonant $\Lambda_c^+ \rightarrow K^+K^-p\pi^0$ decays, respectively.

We use the well-established decay $\Lambda_c^+ \rightarrow pK^-\pi^+$ [17] as the normalization channel for the branching fraction measurements. The track, particle identification, and vertex selection criteria are similar to those used for the signal decays. If there are multiple candidates present in an event, we select the candidate having the smallest value of χ^2 from the Λ_c^+ vertex fit. The resulting invariant mass distribution of the $pK^-\pi^+$ candidates is shown in Fig. 3. The signal is modeled with the sum of three Gaussian functions, and the combinatorial background is modeled with a linear function. There are $1\,468\,435 \pm 4816$ signal candidates and $567\,855 \pm 815$ background candidates in the Λ_c^+ signal region.

The ratio of branching fractions is calculated as

$$\frac{\mathcal{B}(\Lambda_c^+ \rightarrow \text{final state})}{\mathcal{B}(\Lambda_c^+ \rightarrow pK^-\pi^+)} = \frac{Y_{\text{Sig}}/\varepsilon_{\text{Sig}}}{Y_{\text{Norm}}/\varepsilon_{\text{Norm}}}, \quad (2)$$

where Y represents the observed yield in the signal region of the decay of interest and ε corresponds to the reconstruction efficiency as obtained from the MC simulation. For the $\phi p\pi^0$ final state, we include $\mathcal{B}(\phi \rightarrow K^+K^-) = (48.9 \pm 0.5)\%$ [17] in ε_{sig} of Eq. (2). The reconstruction efficiencies are $(2.165 \pm 0.007)\%$, $(2.291 \pm 0.008)\%$, and $(16.564 \pm 0.023)\%$ for $\phi p\pi^0$, nonresonant $K^+K^-p\pi^0$, and $pK^-\pi^+$ final states, respectively, where the errors are due to MC statistics only. The ratio $\varepsilon_{\text{Sig}}/\varepsilon_{\text{Norm}}$ is corrected by a factor 1.028 ± 0.018 to account for small differences in particle identification efficiencies between data and simulation. This correction is estimated from a sample of $D^{*+} \rightarrow D^0(\rightarrow K^-\pi^+)\pi^+$ decays. For the $\phi p\pi^0$ final state, the ratio is

$$\frac{\mathcal{B}(\Lambda_c^+ \rightarrow \phi p\pi^0)}{\mathcal{B}(\Lambda_c^+ \rightarrow pK^-\pi^+)} = (1.538 \pm 0.641_{-0.100}^{+0.077}) \times 10^{-3}.$$

Whenever two or more uncertainties are quoted, the first is statistical and the second is systematic. Using $\mathcal{B}(\Lambda_c^+ \rightarrow pK^-\pi^+) = (6.46 \pm 0.24)\%$ [20], we obtain

$$\mathcal{B}(\Lambda_c^+ \rightarrow \phi p\pi^0) = (9.94 \pm 4.14_{-0.65}^{+0.50} \pm 0.37) \times 10^{-3},$$

where the third uncertainty is that due to the branching fraction $\mathcal{B}(\Lambda_c^+ \rightarrow pK^-\pi^+)$.

Since the significances are below 3.0 standard deviations for both $\phi p\pi^0$ signal and $K^+K^-p\pi^0$ nonresonant decays, we set upper limits on their branching fractions at 90% confidence level (C.L.) using a Bayesian approach.

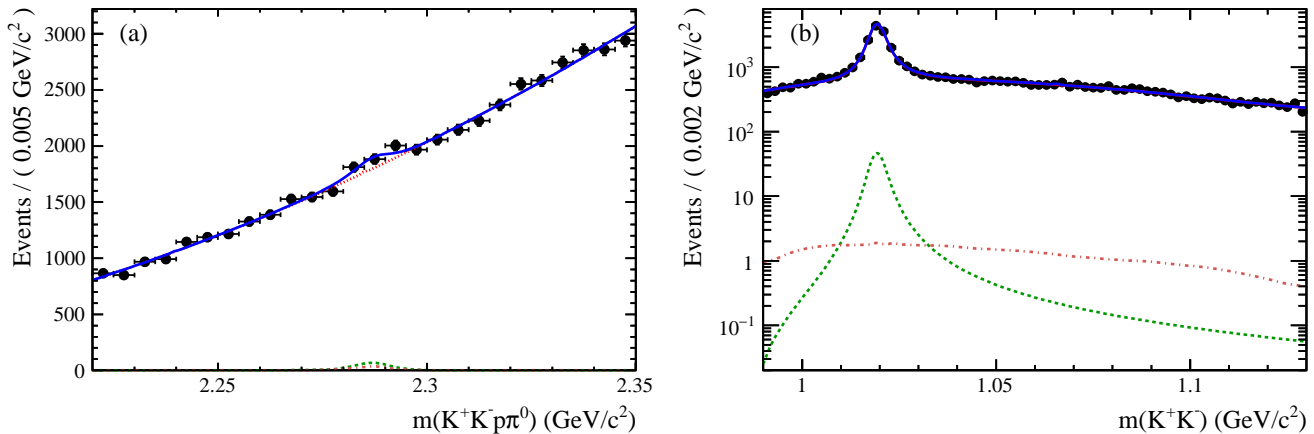


FIG. 2. Projections of the 2D fit: (a) $m(K^+K^-\pi^0)$ and (b) $m(K^+K^-)$. The points with the error bars are the data, and the (red) dotted, (green) dashed and (brown) dot-dashed curves represent the combinatorial, signal and nonresonant candidates, respectively, and (blue) solid curves represent the total PDF. The solid curve in (b) completely overlaps the curve for the combinatorial background.

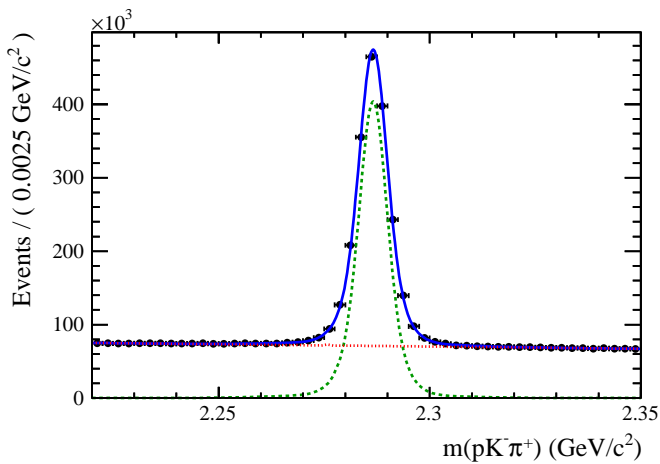


FIG. 3. Fit to the invariant mass distribution of $pK^-\pi^+$. The points with the error bars are the data, the (red) dotted and (green) dashed curves represent the combinatorial and signal candidates, respectively, and (blue) curve represents the total PDF.

The limit is obtained by integrating the likelihood function from zero to infinity; the value that corresponds to 90% of this total area is taken as the 90% C.L. upper limit. We include the systematic uncertainty in the calculation by convolving the likelihood distribution with a Gaussian function whose width is set equal to the total systematic uncertainty. The results are

$$\begin{aligned} \mathcal{B}(\Lambda_c^+ \rightarrow \phi p \pi^0) &< 15.3 \times 10^{-5}, \\ \mathcal{B}(\Lambda_c^+ \rightarrow K^+K^-\pi^0)_{\text{NR}} &< 6.3 \times 10^{-5}, \end{aligned}$$

which are the first limits on these branching fractions.

To search for a putative $P_s^+ \rightarrow \phi p$ decay, we select $\Lambda_c^+ \rightarrow K^+K^-\pi^0$ candidates in which $m(K^+K^-)$ is within $0.020 \text{ GeV}/c^2$ of the ϕ meson mass [17] and plot

the background-subtracted $m(\phi p)$ distribution (Fig. 4). This distribution is obtained by performing 2D fits as discussed above in bins of $m(\phi p)$. The data shows no clear evidence for a P_s^+ state. We set an upper limit on the product branching fraction $\mathcal{B}(\Lambda_c^+ \rightarrow P_s^+\pi^0) \times \mathcal{B}(P_s^+ \rightarrow \phi p)$ by fitting the distribution of Fig. 4 to the sum of a RBW function and a phase space distribution determined from a sample of simulated $\Lambda_c^+ \rightarrow \phi p \pi^0$ decays. We obtain $77.6 \pm 28.1 P_s^+$ events from the fit, which gives an upper limit of

$$\mathcal{B}(\Lambda_c^+ \rightarrow P_s^+\pi^0) \times \mathcal{B}(P_s^+ \rightarrow \phi p) < 8.3 \times 10^{-5}$$

at 90% C.L. This limit is calculated using the same procedure as that used for our limit on $\mathcal{B}(\Lambda_c^+ \rightarrow \phi p \pi^0)$. The systematic uncertainties for the two cases are essentially identical except for that due to the size of the MC sample used to calculate the reconstruction efficiency. The efficiency used here [$\varepsilon = (2.438 \pm 0.026)\%$] corresponds to the fitted values $M_{P_s^+} = (2.025 \pm 0.005) \text{ GeV}/c^2$ and $\Gamma_{P_s^+} = (0.022 \pm 0.012) \text{ GeV}$.

For the $\Lambda_c^+ \rightarrow K^-\pi^+p\pi^0$ sample, the mass distribution is plotted in Fig. 5. We fit this distribution to obtain the signal yield. We model the signal with a sum of two CB functions having a common mean, and the combinatorial background with a linear function. We find 242039 ± 2342 signal candidates and 472729 ± 467 background candidates in the Λ_c^+ signal region. The corresponding signal efficiency is $(3.988 \pm 0.009)\%$, obtained from MC simulation. We measure the ratio of branching fractions

$$\frac{\mathcal{B}(\Lambda_c^+ \rightarrow K^-\pi^+p\pi^0)}{\mathcal{B}(\Lambda_c^+ \rightarrow K^-\pi^+p)} = (0.685 \pm 0.007 \pm 0.018),$$

which results in a branching fraction

$$\mathcal{B}(\Lambda_c^+ \rightarrow K^-\pi^+p\pi^0) = (4.42 \pm 0.05 \pm 0.12 \pm 0.16)\%.$$

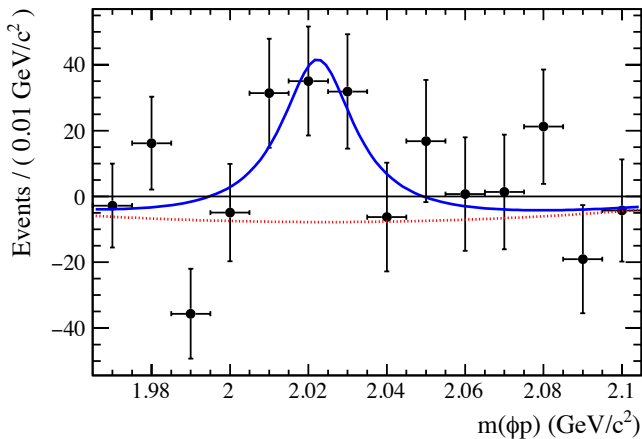


FIG. 4. The background-subtracted distribution of $m(\phi p)$ in the $\phi p \pi^0$ final state. The points with error bars are data, and the (blue) solid line shows the total PDF. The (red) dotted curve shows the fitted phase space component (which has fluctuated negative).

This is the most precise measurement of $\mathcal{B}(\Lambda_c^+ \rightarrow K^- \pi^+ p \pi^0)$ to date and is consistent with the recently measured value $\mathcal{B}(\Lambda_c^+ \rightarrow K^- \pi^+ p \pi^0) = (4.53 \pm 0.23 \pm 0.30)\%$ by the BESIII collaboration [21].

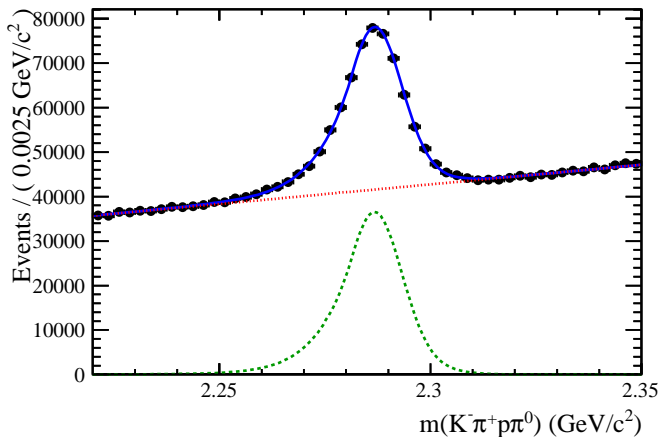


FIG. 5. Fit to the invariant mass distribution of $m(K^- \pi^+ p \pi^0)$. The points with the error bars are the data, the (red) dotted and (green) dashed curves represent the combinatorial and signal candidates, respectively, and (blue) curve represents the total PDF. The $\chi^2 / (\text{number of bins})$ of the fit is 1.43, which indicate that the fit gives a good description of the data.

The systematic uncertainties on all branching fractions are listed in Table I. The uncertainties due to fixed parameters in the PDF shape are estimated by varying the parameters individually according to their statistical uncertainties. For each variation, the branching fraction is recalculated, and the difference with the nominal value is taken as the systematic uncertainty associated

with that parameter. In order to determine the systematic uncertainty due to the $m(K^+ K^-)$ PDF of nonresonant $K^+ K^- p \pi^0$, we replace the nonparametric PDF by a fourth-order polynomial and refit the data. For the $\phi p \pi^0$ final state, we also try including a separate PDF for an $f_0(980)$ intermediate state. The differences in the fit results are included as systematic uncertainties. We add all uncertainties in quadrature to obtain the overall uncertainty due to PDF parametrization. The uncertainties due to errors in the calibration factors used to account for small data-MC differences in the signal PDF are evaluated separately but in a similar manner. A systematic uncertainty of -1.2% is assigned to account for changes associated with the choice of the $m(K^+ K^-)$ range in $\mathcal{B}(\Lambda_c^+ \rightarrow \phi p \pi^0)$. A 2.1% systematic uncertainty is assigned due to the best candidate selection. This is evaluated by analyzing the decay channel $\Lambda_c^+ \rightarrow \Sigma^+ \phi$, which has much higher purity than the signal channels analyzed. We determine this by applying an alternative best candidate selection, *i.e.*, the deviations of the candidate ϕ and Σ^+ masses from their nominal values. The difference in the branching fraction due to the two methods of the best candidate selection is taken as the systematic uncertainty. We assign a 1.5% systematic uncertainty due to π^0 reconstruction; this is determined from a study of $\tau^- \rightarrow \pi^- \pi^0 \nu_\tau$ decays. Since the branching fractions are measured with respect to the normalization channel $\Lambda_c^+ \rightarrow p K^- \pi^+$, which has an identical number of charged tracks, the systematic uncertainty due to differences in tracking performance between signal and normalization modes is negligible. There is a 1.8% systematic uncertainty assigned for the particle identification efficiencies in the $\phi p \pi^0$ and nonresonant $K^+ K^- p \pi^0$ final states relative to the $p K^- \pi^+$ normalization channel. The uncertainty in acceptance due to possible resonance substructure in the decay is found to be negligible. The total of the above systematic uncertainties is calculated as their sum in quadrature. In addition, there is a 3.7% uncertainty due to the branching fraction of the normalization mode. As this large uncertainty does not arise from our analysis and will decrease with future measurements of $\Lambda_c^+ \rightarrow p K^- \pi^+$, we quote it separately.

In summary, we have searched for the decays $\Lambda_c^+ \rightarrow \phi p \pi^0$ and nonresonant $\Lambda_c^+ \rightarrow K^+ K^- p \pi^0$. No significant signal is observed for either decay mode and we set 90% C.L. upper limits on their branching fractions, which are $\mathcal{B}(\Lambda_c^+ \rightarrow \phi p \pi^0) < 15.3 \times 10^{-5}$ and $\mathcal{B}(\Lambda_c^+ \rightarrow K^+ K^- p \pi^0)_{\text{NR}} < 6.3 \times 10^{-5}$. We see no evidence for a hidden-strangeness pentaquark decay $P_s^+ \rightarrow \phi p$ and set an upper limit on the product branching fraction of $\mathcal{B}(\Lambda_c^+ \rightarrow P_s^+ \pi^0) \times \mathcal{B}(P_s^+ \rightarrow \phi p) < 8.3 \times 10^{-5}$ at 90% C.L. This limit is a factor of six higher than the product branching fraction measured by LHCb for an analogous hidden-charm pentaquark state: $\mathcal{B}(\Lambda_b^0 \rightarrow P_c(4450)^+ K^-) \times \mathcal{B}(P_c(4450)^+ \rightarrow J/\psi p) = (1.3 \pm 0.4) \times 10^{-5}$ [3]. We also measure $\mathcal{B}(\Lambda_c^+ \rightarrow K^- \pi^+ p \pi^0) =$

TABLE I. Systematic uncertainties (%) on $\mathcal{B}(\Lambda_c^+ \rightarrow \phi p \pi^0)$, $\mathcal{B}(\Lambda_c^+ \rightarrow K^+ K^- p \pi^0)_{\text{NR}}$, and $\mathcal{B}(\Lambda_c^+ \rightarrow K^- \pi^+ p \pi^0)$.

Source	$\mathcal{B}(\Lambda_c^+ \rightarrow \phi p \pi^0)$	$\mathcal{B}(\Lambda_c^+ \rightarrow K^+ K^- p \pi^0)_{\text{NR}}$	$\mathcal{B}(\Lambda_c^+ \rightarrow K^- \pi^+ p \pi^0)$
PDF parametrization	+1.0 -1.9	+1.9 -1.5	-
Calibration factor	+3.8 -5.2	+2.8 -1.5	-
Choice of $m(K^+ K^-)$ range	+0.0 -1.2	-	-
Best candidate selection	2.1	2.1	2.1
MC sample size	0.4	0.4	0.3
π^0 reconstruction	1.5	1.5	1.5
Particle identification	1.8	1.8	-
$\mathcal{B}(\phi \rightarrow K^+ K^-)$	1.0	-	-
Total (without $\mathcal{B}_{\text{Norm}}$)	+5.0 -6.5	+4.6 -3.8	2.6
$\mathcal{B}_{\text{Norm}}$	3.7	3.7	3.7

$(4.42 \pm 0.05 \pm 0.12 \pm 0.16)\%$. This is the world's most precise measurement of this branching fraction.

ACKNOWLEDGMENTS

We thank the KEKB group for the excellent operation of the accelerator; the KEK cryogenics group for the efficient operation of the solenoid; and the KEK computer group, the National Institute of Informatics, and the PNNL/EMSL computing group for valuable computing and SINET5 network support. We acknowledge support from the Ministry of Education, Culture, Sports, Science, and Technology (MEXT) of Japan, the Japan Society for the Promotion of Science (JSPS), and the Tau-Lepton Physics Research Center of Nagoya University; the Australian Research Council; Austrian Science Fund under Grant No. P 26794-N20; the National Natural Science Foundation of China under Contracts No. 10575109, No. 10775142, No. 10875115, No. 11175187, No. 11475187, No. 11521505 and No. 11575017; the Chinese Academy of Science Center for Excellence in Particle Physics; the Ministry of Education, Youth and Sports of the Czech Republic under Contract No. LTT17020; the Carl Zeiss Foundation, the Deutsche Forschungsgemeinschaft, the Excellence Cluster Universe, and the VolkswagenStiftung; the Department of Science and Technology of India; the Istituto Nazionale di Fisica Nucleare of Italy; the WCU program of the Ministry of Education, National Research Foundation (NRF) of Korea Grants No. 2011-0029457, No. 2012-0008143, No. 2014R1A2A2A01005286, No. 2014R1A2A2A01002734, No. 2015R1A2A2A01003280, No. 2015H1A2A1033649, No. 2016R1D1A1B01010135, No. 2016K1A3A7A09005603, No. 2016K1A3A7A09005604, No. 2016R1D1A1B02012900, No. 2016K1A3A7A09005606, No. NRF-2013K1A3A7A06056592; the Brain Korea 21-Plus program, Radiation Science Research Institute, Foreign Large-size Research Facility Application Supporting

project and the Global Science Experimental Data Hub Center of the Korea Institute of Science and Technology Information; the Polish Ministry of Science and Higher Education and the National Science Center; the Ministry of Education and Science of the Russian Federation and the Russian Foundation for Basic Research; the Slovenian Research Agency; Ikerbasque, Basque Foundation for Science and MINECO (Juan de la Cierva), Spain; the Swiss National Science Foundation; the Ministry of Education and the Ministry of Science and Technology of Taiwan; and the U.S. Department of Energy and the National Science Foundation.

-
- [1] S. K. Choi *et al.* (Belle Collaboration), Observation of a narrow charmoniumlike state in exclusive $B^\pm \rightarrow K^\pm \pi^+ \pi^- J/\psi$ decays, *Phys. Rev. Lett.* **91**, 262001 (2003).
 - [2] C. Patrignani *et al.* (Particle Data Group), Review of particle physics, *Spectroscopy of mesons containing two heavy quarks*, *Chin. Phys. C* **40**, 100001 (2016).
 - [3] R. Aaij *et al.* (LHCb Collaboration), Observation of $J/\psi p$ resonances consistent with pentaquark states in $\Lambda_b^0 \rightarrow J/\psi K^- p$ decays, *Phys. Rev. Lett.* **115**, 072001 (2015).
 - [4] R. Zhu and C. F. Qiao, Pentaquark states in a diquark-triquark model, *Phys. Lett. B* **756**, 259 (2016).
 - [5] V. Kopeliovich and I. Potashnikova, Simple estimates of the hidden beauty pentaquarks masses, arXiv:1510.05958 [hep-ph].
 - [6] R. F. Lebed, Do the P_c^+ pentaquarks have strange siblings?, *Phys. Rev. D* **92**, 114030 (2015).
 - [7] Unless stated otherwise, charge-conjugate modes are implicitly included.
 - [8] T. Mibe *et al.* (LEPS Collaboration), Diffractive ϕ -meson photoproduction on proton near threshold, *Phys. Rev. Lett.* **95**, 182001 (2005).
 - [9] B. Dey *et al.* (CLAS Collaboration), Data analysis techniques, differential cross sections, and spin density matrix elements for the reaction $\gamma p \rightarrow \phi p$, *Phys. Rev. C* **89**, 055208 (2014); *Phys. Rev. C* **90**, 019901 (2014).
 - [10] R. F. Lebed, Diquark substructure in ϕ photoproduction, *Phys. Rev. D* **92**, 114006 (2015).

- [11] A. Abashian *et al.* (Belle Collaboration), The Belle Detector, Nucl. Instrum. Methods Phys. Res., Sect. A **479**, 117 (2002); also see the detector section in J. Brodzicka *et al.*, Physics achievements from the Belle Experiment, Prog. Theor. Exp. Phys. **2012**, 04D001 (2012).
- [12] S. Kurokawa and E. Kikutani, Overview of the KEKB accelerators, Nucl. Instrum. Methods Phys. Res. Sect. A **499**, 1 (2003), and other papers included in this volume. T.Abe *et al.*, Achievements of KEKB, Prog. Theor. Exp. Phys. **2013**, 03A001 (2013) and references therein.
- [13] D. J. Lange, The EVTGEN particle decay simulation package, Nucl. Instrum. Methods Phys. Res., Sect. A **462**, 152 (2001).
- [14] T. Sjöstrand, High-energy physics event generation with PYTHIA 5.7 and JETSET 7.4, Comput. Phys. Commun. **82** 74 (1994).
- [15] R. Brun *et al.*, GEANT 3.21, CERN Report DD/EE/84-1, 1984.
- [16] E. Barberio and Z. Was, PHOTOS: A universal Monte Carlo for QED radiative corrections. Version 2.0, Comput. Phys. Commun. **79**, 291 (1994).
- [17] C. Patrignani *et al.* (Particle Data Group), Review of particle physics, Chin. Phys. C **40**, 100001 (2016).
- [18] T. Skwarnicki, A study of the radiative CASCADE transitions between the Upsilon-prime and Upsilon resonances, DESY-F31-86-02.
- [19] K. S. Cranmer, Kernel estimation in high-energy physics, Comput. Phys. Commun. **136**, 198 (2001).
- [20] Y. Amhis *et al.* (Heavy Flavor Averaging Group), Averages of b -hadron, c -hadron, and τ -lepton properties as of summer 2016, arXiv:1612.07233 [hep-ex].
- [21] M. Ablikim *et al.* (BESIII Collaboration), Measurements of absolute hadronic branching fractions of the Λ_c^+ baryon, Phys. Rev. Lett. **116**, 052001 (2016).